

Time-dependent Hartree-Fock plus Langevin approach for hot fusion reactions to synthesize the $Z = 120$ superheavy element

K. Sekizawa¹ and K. Hagino^{2,3}

¹Center for Transdisciplinary Research, Institute for Research Promotion, Niigata University, Niigata 950-2181, Japan

²Department of Physics, Tohoku University, Sendai 980-8578, Japan

³Research Center for Electron Photon Science, Tohoku University, 1-2-1 Mikamine, Sendai 982-0826, Japan



(Received 15 March 2019; published 22 May 2019)

We develop a novel approach to fusion reactions for synthesis of superheavy elements, which combines the time-dependent Hartree-Fock (TDHF) method with a dynamical diffusion model based on the Langevin equation. In this approach, the distance of the closest approach for the capture process is estimated within the TDHF approach, which is then plugged into the dynamical diffusion model as an initial condition. We apply this approach to hot fusion reactions leading to formation of the element $Z = 120$, that is, the $^{48}\text{Ca} + ^{254,257}\text{Fm}$, $^{51}\text{V} + ^{249}\text{Bk}$, and $^{54}\text{Cr} + ^{248}\text{Cm}$ reactions. Our calculations indicate that the distances of the closest approach for these systems are similar to each other and thus the difference in the probabilities of evaporation residue formation among those reaction systems originates mainly from the evaporation process, which is sensitive to the fission barrier height and the excitation energy of a compound nucleus.

DOI: [10.1103/PhysRevC.99.051602](https://doi.org/10.1103/PhysRevC.99.051602)

The physics of superheavy elements is one of the most important topics in nuclear physics today [1–6]. Using heavy-ion fusion reactions, researchers have so far successfully synthesized the elements up to $Z = 118$ [3]. Since the formation probability of superheavy elements is extremely small, it is crucial to choose an appropriate reaction system, that is, a combination of projectile and target nuclei. For this purpose, two different experimental strategies have been employed. One is the ^{208}Pb -based cold fusion reactions, for which the compound nucleus is formed with relatively low excitation energies so that the survival probability of the compound nucleus against fission is maximized. The other is the ^{48}Ca -based hot fusion reactions, for which the formation probability of the compound nucleus is maximized.

It has been shown that the evaporation residue cross sections associated with the cold fusion reactions drop rapidly as the charge number Z of the compound nucleus increases. Because of this behavior, the cold fusion reactions have been limited only up to nihonium ($Z = 113$) [7]. On the other hand, the observed cross sections remain relatively large between $Z = 113$ and 118 for hot fusion reactions [2]. It has been conjectured that this behavior originates from the fact that the compound nuclei formed are in the proximity of the island of stability [8,9] and/or an increase of dissipation at high temperatures [10]. For this reason, the hot fusion reactions are regarded as a promising means to go beyond the known heaviest element, oganesson ($Z = 118$), and synthesize new superheavy elements.

To synthesize the new elements, $Z = 119$ and 120, with hot fusion reactions utilizing the ^{48}Ca projectile as in the previous successful measurements, use of Es ($Z = 99$) and Fm ($Z = 100$) targets is mandatory. However, due to the short half-lives of these elements, they would not be available with

sufficient amounts for fusion experiments [11]. It is therefore inevitable to use heavier projectile nuclei, such as ^{50}Ti , ^{51}V , and ^{54}Cr , instead of ^{48}Ca . An important question arises: how much are evaporation residue cross sections altered if those heavier projectiles are used instead of the ^{48}Ca nucleus? In particular, one may ask how the double magic nature of ^{48}Ca influences the evaporation residue cross sections.

The role of magicity in fusion reactions has been demonstrated in Ref. [12] for the $^{86}\text{Kr} + ^{138}\text{Ba}$ and $^{86}\text{Kr} + ^{134}\text{Ba}$ systems. In this experiment, it was shown that the cross sections for the former system are systematically larger than those for the latter. An interpretation of this behavior is that the projectile nucleus can come closer to the target nucleus with less friction in the former system, in which the target nucleus has the $N = 82$ magic number. See also Ref. [13] for single-particle energies for the $^{70}\text{Zn} + ^{208}\text{Pb}$ system as a function of the internucleus distance. We also mention that a recent experiment for the $^{50,52,54}\text{Cr} + ^{204,206,208}\text{Pb}$ systems [14] clearly showed that fusion cross sections can be enhanced by the entrance-channel magicity provided that the N/Z asymmetry is small, as discussed in Ref. [15]. It may be natural to expect that the ^{48}Ca nucleus maintains a similar effect as well.

To address this question, one would need a microscopic approach based on the nucleonic degrees of freedom with minimal assumptions on dynamics. The aim of this paper is to develop a new hybrid model based on such a microscopic approach, for which we employ the time-dependent Hartree-Fock (TDHF) theory. The TDHF approach is free from empirical parameters once the energy density functional is fixed from nuclear structure calculations. In recent years, the TDHF approach has been extensively applied to heavy-ion reactions around the Coulomb barrier (see, e.g., Refs. [16–20] for recent reviews). Of course, the TDHF approach is valid only for the

main process in a reaction [20,21], and we cannot expect that the TDHF approach is able to describe the entire formation process of evaporation residues of superheavy elements. We mention that one of the main processes in fusion for syntheses of superheavy elements is quasifission, which is a reparation of the two colliding nuclei before the compound nucleus formation. It has been shown that the TDHF approach is applicable for its description, at least for its average behavior [22–25]. The main idea of the hybrid approach developed in this paper is to extract the distance of the closest approach from such calculations, and use it as an initial condition of the diffusion process over the inner barrier, for which the Langevin approach has been developed [26–29]. We shall apply this new approach to fusion reactions to form the element $Z = 120$, and clarify the role of the magicity of the ^{48}Ca projectile in fusion reactions for superheavy elements.

Conceptually, the formation process of evaporation residues can be divided into the following three subprocesses [26–29]. The first is the capture process, in which the projectile and target nuclei come close to the touching configuration. The second is the diffusion process, in which the touching configuration undergoes the shape evolution toward the compound nucleus by overcoming an inner barrier. At this stage, there is a strong competition between this diffusion process and the reparation, i.e., quasifission. The third process is the statistical decay of the compound nucleus, in which there is a severe competition between evaporation and fission. Cross sections for the formation of evaporation residues are then given as a product of the probability of each of these three processes, that is,

$$\sigma_{\text{ER}}(E) = \frac{\pi}{k^2} \sum_l (2l+1) T_l(E) P_{\text{CN}}(E, l) W_{\text{sur}}(E^*, l), \quad (1)$$

where l is a partial wave, E is the incident energy in the center-of-mass frame, and k is given by $k = \sqrt{2\mu E}/\hbar$ with μ being the reduced mass in the entrance channel. T_l , P_{CN} , and W_{sur} are the probabilities for the first, second, and third processes, respectively. The survival probability W_{sur} is a function of the excitation energy E^* and the angular momentum l of the compound nucleus. In the following, to compare the several systems, we focus only on the s -wave scattering (i.e., $l = 0$) and take the energy E to be above the Coulomb barrier so that the capture probability T_l can be set to unity.

We first compare the $^{54}\text{Cr} + ^{248}\text{Cm}$ and $^{48}\text{Ca} + ^{254}\text{Fm}$ systems, both of which lead to the same compound nucleus, $^{302}120$, even though the ^{254}Fm nucleus is short lived and it cannot be used as the target nucleus in an actual experiment. The first step in our approach is to perform the TDHF calculation for a head-on collision, $b = 0$. For TDHF calculations, we use the three-dimensional TDHF code developed by Sekizawa and Yabana (see, e.g., Refs. [25,30–32] for details of the numerical implementation). For the energy density functional, we use the Skyrme SLy4d parameter set [33]. The pairing correlations are disregarded in this work. To obtain a spherical ground state, the filling approximation is employed for ^{54}Cr , filling proton $f_{7/2}$ and neutron $p_{3/2}$ orbitals with equal weights for the magnetic substates. The ^{248}Cm and ^{254}Fm nuclei are prolately deformed in their ground state. Since a dominant

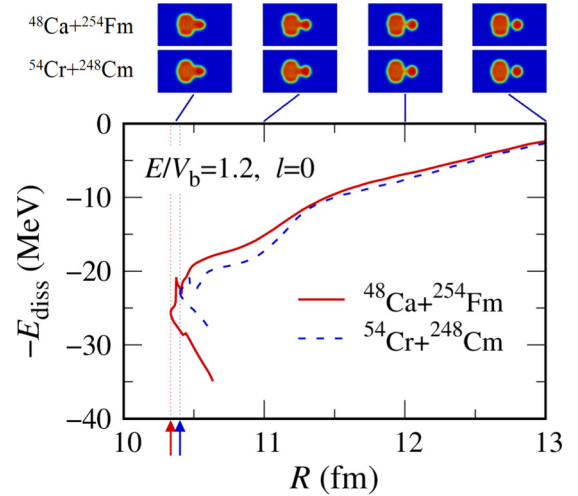


FIG. 1. Results of the TDHF calculations (with the SLy4d functional [33]) for the energy loss for the relative motion between the projectile and target nuclei, shown as a function of the internucleus distance R . The solid and dashed lines are for the $^{48}\text{Ca} + ^{254}\text{Fm}$ and $^{54}\text{Cr} + ^{248}\text{Cm}$ reactions, respectively, for the s -wave scattering ($l = 0$) with the side collision geometry. The incident energy is set to be 1.2 times the Coulomb barrier height for the side collision, which is evaluated with the frozen Hartree-Fock approximation. The arrows and vertical dotted lines indicate the distance of the closest approach for each system. At the top of the figure, the density distribution in the reaction plane is exhibited for $^{48}\text{Ca} + ^{254}\text{Fm}$ (the top row) and $^{54}\text{Cr} + ^{248}\text{Cm}$ (the bottom row). Each panel corresponds to a different instance at which the relative distance is $R = R_{\text{min}}$, 11, 12, and 13 fm, respectively, from left to right.

contribution to evaporation residue cross sections comes from the side collision [34–40], for which the projectile nucleus collides with the equatorial side of the target, for simplicity we restrict our calculations only to this configuration in the present paper.

Following Ref. [41], we extract from the TDHF time evolution the relative distance $R(t)$ between the two fragments, its conjugate momentum $P(t)$, the reduced mass $\mu(R(t))$, the internucleus potential $V(R(t))$, and the friction coefficient $\gamma(R(t))$, as a function of time t . Having these quantities at hand, we can compute the energy for the relative motion

$$E_{\text{rel}}(R(t)) = \frac{P(t)^2}{2\mu(R(t))} + V(R(t)). \quad (2)$$

Notice that because of internal excitations, the energy is dissipated from the relative motion to internal degrees of freedom. Figure 1 shows the minus of the dissipative energy E_{diss} , which is nothing but the relative energy with respect to the initial energy E for these systems as a function of the relative distance R . The initial energy is set to 1.2 times the Coulomb barrier height for the side collision. Here, the barrier height V_b is estimated using the frozen Hartree-Fock method [42]. This yields $V_b = 212.8$ and 243.2 MeV for the $^{48}\text{Ca} + ^{254}\text{Fm}$ and $^{54}\text{Cr} + ^{248}\text{Cm}$ systems, respectively. Notice that the actual threshold energies for fusion are somewhat smaller than these values due to the dynamical modifications of the barriers [43–47]. The figure also shows the density distributions for

each system at $R = R_{\min}$, 11, 12, and 13 fm, where R_{\min} is the distance of the closest approach. The figure indicates that the energy loss in the approaching phase is indeed larger for the $^{54}\text{Cr} + ^{248}\text{Cm}$ system than for the $^{48}\text{Ca} + ^{254}\text{Fm}$ system. However, the distance of the closest approach, R_{\min} , does not differ much, that is, $R_{\min} = 10.33$ and 10.40 fm for the $^{48}\text{Ca} + ^{254}\text{Fm}$ and $^{54}\text{Cr} + ^{248}\text{Cm}$ systems, respectively, for the case of $E = 1.2V_b$ (see the arrows in Fig. 1). At $E = V_b$, the distance of the closest approach is $R_{\min} = 12.93$ and 13.09 fm for the former and the latter systems, respectively. This implies that the magicity of the ^{48}Ca nucleus plays a minor role in determining the distance of the closest approach, even though it significantly affects the dynamics before the touching.

Here, we mention that the discontinuity in the energy loss at small relative distances shown in Fig. 1 is due to a tiny jump of a neck position, which causes a discontinuity in $V(R(t))$ and $\gamma(R(t))$ through a numerical time derivative. Even though we may remedy it by improving the neck detection algorithm, the conclusion of the present paper will be maintained, as it does not change much the value of R_{\min} .

Let us next evaluate the diffusion probability P_{CN} and the survival probability W_{sur} in Eq. (1) using the distances of the closest approach evaluated with the TDHF calculations. To this end, we employ the fusion-by-diffusion model [27,40,48,49]. In this model, the diffusion process is described as diffusion over a simple one-dimensional parabolic potential from an injection point [50], while the decay of the compound nucleus is described with a simplified statistical model in which only the competitions between fission and neutron evaporations are taken into account. In the overdamped regime assumed in the fusion-by-diffusion model, the diffusion probability depends only on the temperature and height of the inner barrier [27,50]. Therefore, after a mass formula, a level density parameter, and a parametrization of the inner barrier are specified, there remains only a single adjustable parameter, i.e., the injection point parameter, which defines the effective height of the inner barrier. We estimate the injection point parameter as

$$s_{\text{inj}} = R_{\min} - R_{\text{P}} - R_{\text{T}}, \quad (3)$$

where R_{\min} is the distance of the closest approach obtained from the TDHF calculations, while R_{P} and R_{T} are the radii of the projectile and the target nuclei, respectively. In this paper, we use 1.15 fm for the radius parameter. The explicit form of the inner barrier is given in Ref. [48], for which we use the default parameter set. Notice that the deformation effect is taken into account in the extended fusion-by-diffusion model through the orientation angle dependence of R_{\min} , while the inner potential remains independent of the orientation angle [40]. We also assume that the kinetic energy is completely dissipated to the internal energy at the injection point. See Refs. [27,40,48,49] for other details of the fusion-by-diffusion model.

Table I summarizes the diffusion and survival probabilities evaluated at $E = V_b$. Here, the survival probabilities represent the total survival probabilities, which are a sum of probabilities for all neutron evaporation channels. Following Refs. [40,49], we use the mass formula and the fission barrier

TABLE I. The diffusion probability P_{CN} , the survival probability W_{sur} , and their product $P_{\text{CN}}W_{\text{sur}}$, estimated with the fusion-by-diffusion model for several hot fusion reactions leading to the element 120. These quantities are evaluated for the s -wave scattering at $E = V_b$ for the side collision for each reaction. The excitation energy E^* of the compound nucleus (CN) as well as the distance of the closest approach estimated with the TDHF calculations are also shown.

System	CN	E^* (MeV)	R_{\min} (fm)	P_{CN} ($\times 10^4$)	W_{sur} ($\times 10^9$)	$P_{\text{CN}}W_{\text{sur}}$ ($\times 10^{13}$)
$^{48}\text{Ca} + ^{254}\text{Fm}$	$^{302}120$	29.0	12.93	1.72	176	302
$^{54}\text{Cr} + ^{248}\text{Cm}$	$^{302}120$	33.2	13.09	1.89	1.31	2.47
$^{51}\text{V} + ^{249}\text{Bk}$	$^{300}120$	37.0	12.94	3.95	0.117	0.461
$^{48}\text{Ca} + ^{257}\text{Fm}$	$^{305}120$	30.5	12.94	2.49	0.729	1.82

heights given in Ref. [51]. This mass formula predicts the fusion Q values of $Q_{\text{fus}} = -183.8$ and -210.10 MeV for the $^{48}\text{Ca} + ^{254}\text{Fm}$ and the $^{54}\text{Cr} + ^{248}\text{Cm}$ systems, respectively, and thus the excitation energy of the compound nucleus formed at $E = V_b$ in the former reaction is smaller than that formed in the latter reaction. Because the distances of the closest approach are similar to each other, the diffusion probability P_{CN} for the $^{54}\text{Cr} + ^{248}\text{Cm}$ reaction is slightly larger than that for the $^{48}\text{Ca} + ^{254}\text{Fm}$ reaction, reflecting the higher excitation energy. On the other hand, the survival probability W_{sur} is much more sensitive to the excitation energy, and that for the $^{48}\text{Ca} + ^{254}\text{Fm}$ reaction is larger than that for the $^{54}\text{Cr} + ^{248}\text{Cm}$ reaction by about two orders of magnitude. The products of the diffusion and survival probabilities are also different by a similar amount. This clearly indicates that the main effect of the magicity of the ^{48}Ca nucleus is due to the low excitation energies of the compound nucleus, whereas the dynamics of the entrance channel plays a much less important role. This is in contrast to the cases with heavy magic nuclei, for which the magicity plays an important role in the entrance channel dynamics [12,13].

We next discuss the projectile-target combinations which are experimentally accessible, namely, the $^{54}\text{Cr} + ^{248}\text{Cm} \rightarrow ^{302}120$ and the $^{51}\text{V} + ^{249}\text{Bk} \rightarrow ^{300}120$ systems. For comparison, we also consider the ^{48}Ca -induced reaction with ^{257}Fm , which is the longest lived Fm isotope (with the half-life of 100.5 days), that is, $^{48}\text{Ca} + ^{257}\text{Fm} \rightarrow ^{305}120$. The energy losses for the relative motion at $E = 1.2V_b$ evaluated with the TDHF calculations are shown in Fig. 2 for these three systems. For the ^{51}V nucleus, we apply the filling approximation for protons in the $f_{7/2}$ orbitals in order to obtain a spherical ground state. The barrier heights are estimated to be $V_b = 237.0$ and 212.4 MeV for the $^{51}\text{V} + ^{249}\text{Bk}$ and the $^{48}\text{Ca} + ^{257}\text{Fm}$ systems, respectively. The energy losses for these systems are qualitatively the same as those shown in Fig. 1. That is, even though the energy loss for the ^{48}Ca -induced reaction is somewhat lower than the energy losses for the other two reactions, the distances of the closest approach are similar to each other among the three systems. The distance of the closest approach is estimated to be 10.25, 10.30, and 10.40 fm for the $^{48}\text{Ca} + ^{257}\text{Fm}$, the $^{51}\text{V} + ^{249}\text{Bk}$, and the $^{54}\text{Cr} + ^{248}\text{Cm}$

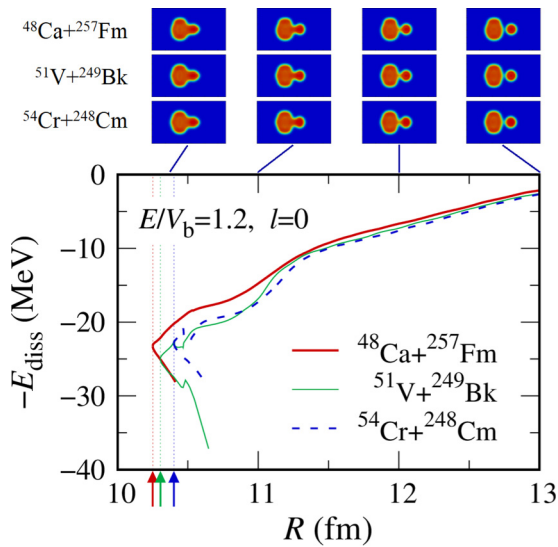


FIG. 2. Same as Fig. 1, but for the $^{48}\text{Ca} + ^{257}\text{Fm}$ (thick solid line), the $^{51}\text{V} + ^{249}\text{Bk}$ (thin solid line), and the $^{54}\text{Cr} + ^{248}\text{Cm}$ (dashed line) systems.

systems, respectively. The distances of the closest approach evaluated at $E = V_b$ are also summarized in Table I.

The diffusion and the survival probabilities for $E = V_b$ for each system are shown in Table I. The small total probability $P_{\text{CN}}W_{\text{sur}}$ for the ^{51}V -induced reaction is caused by the high excitation energy for this system. In addition, an interesting observation is that the survival probability for the $^{48}\text{Ca} + ^{257}\text{Fm}$ reaction is smaller than that for the $^{54}\text{Cr} + ^{248}\text{Cm}$ reaction by a factor of about 1.8 despite the fact that the excitation energy is smaller by about 3 MeV. This is in marked contrast to the comparison to the $^{48}\text{Ca} + ^{254}\text{Fm}$ reaction, for which the low excitation energy (by about 4 MeV) enhances the survival probability by about two orders of magnitude. This difference originates mainly from the mass number dependence of the fission barrier height. The fission barrier heights for the element $Z = 120$ evaluated in Ref. [51] are 5.04, 4.66, and 3.54 MeV for $A = 300$ ($^{51}\text{V} + ^{249}\text{Bk}$), 302 ($^{54}\text{Cr} + ^{248}\text{Cm}$ and $^{48}\text{Ca} + ^{254}\text{Fm}$), and 305 ($^{48}\text{Ca} + ^{257}\text{Fm}$), respectively (Ref. [51] provides the results for even-even nuclei only, and for the $^{305}120$ nucleus we have taken an average of the fission barrier heights for $A = 304$ and 306). That is, the fission barrier height for the compound nucleus formed in the $^{48}\text{Ca} + ^{257}\text{Fm}$ reaction is low, leading to the low survival probability. This again implies that the magicity of the ^{48}Ca nucleus plays a minor role in the entrance channel dynamics in reactions forming superheavy elements.

In summary, we have developed a novel approach for fusion reactions for superheavy elements. This combines good aspects of the microscopic time-dependent Hartree-Fock (TDHF) method and a phenomenological Langevin approach for the diffusion process over the inner barrier: we have used the TDHF approach for the entrance channel dynamics

in order to estimate the distance of the closest approach without an empirical parameter, which provides the initial condition for the Langevin approach. We have applied this new approach to several systems which lead to synthesis of the element 120, i.e., $^{48}\text{Ca} + ^{254,257}\text{Fm}$, $^{51}\text{V} + ^{249}\text{Bk}$, and $^{54}\text{Cr} + ^{248}\text{Cm}$ reactions. We have shown that the distances of the closest approach are similar to one another as long as the incident energy relative to the Coulomb barrier height for each system is kept to be the same. The magicity of the ^{48}Ca nucleus thus influences mainly the evaporation process through the excitation energies of the compound nuclei. We have found that the formation probability of evaporation residues for $^{48}\text{Ca} + ^{254}\text{Fm} \rightarrow ^{302}120$ is larger than that for $^{54}\text{Cr} + ^{248}\text{Cm} \rightarrow ^{302}120$ by about two orders of magnitude. On the other hand, the probability for the latter reaction is larger than that for $^{51}\text{V} + ^{249}\text{Bk} \rightarrow ^{300}120$ by a factor of about 5, reflecting the difference in the excitation energies of the compound nuclei. Despite the magicity of the ^{48}Ca projectile, the probability for the $^{48}\text{Ca} + ^{257}\text{Fm} \rightarrow ^{305}120$ reaction has been found to be slightly smaller than that for the $^{54}\text{Cr} + ^{248}\text{Cm} \rightarrow ^{302}120$ reaction, due to a low fission barrier height of the $^{305}120$ nucleus.

In this paper, for simplicity, we have considered only the s -wave scattering for the side collision geometry. In order to compute evaporation residue cross sections, one would need to add contributions of other partial waves and also to take an average over the orientation angles of the deformed target nuclei. We would, however, not expect that our conclusions in this paper will be altered qualitatively. Also, we have neglected the pairing correlations in the TDHF calculations. The pairing correlations may affect reaction dynamics, especially for the cases with open-shell projectiles, e.g., ^{50}Ti , ^{51}V , and ^{54}Cr , in a way as was discussed recently in Refs. [52,53]. This is completely an open issue, which should be addressed separately in the future. Another simplification which we have taken in this paper is that we have used a simple fusion-by-diffusion model for the diffusion process. This can be improved by using more sophisticated Langevin calculations. We are currently working on this, and we will report it in a separate publication. Another interesting application of the present approach is to the ^{208}Pb -based cold fusion reactions, for which the magicity of the ^{208}Pb nucleus plays an important role in the entrance channel dynamics. We leave it for a future work.

We thank K. Washiyama and Y. Aritomo for useful discussions. This work used computational resources of the HPCI system (Oakforest PACS) provided by the Joint Center for Advanced High Performance Computing (JCAHPC) through the HPCI System Research Projects (Project No. hp180080). This work also used (in part) computational resources of the Cray XC40 System at Yukawa Institute for Theoretical Physics (YITP), Kyoto University and the COMA (PACS-IX) System provided by Multidisciplinary Cooperative Research Program in Center for Computational Sciences, University of Tsukuba.

- [1] S. Hofmann and G. Münzenberg, *Rev. Mod. Phys.* **72**, 733 (2000).
- [2] J. H. Hamilton, S. Hofmann, and Y. T. Oganessian, *Ann. Rev. Nucl. Part. Sci.* **63**, 383 (2013).
- [3] *Special Issue on Superheavy Nuclei*, edited by C. E. Düllmann, R.-D. Herzberg, W. Nazarewicz, and Y. Oganessian, *Nucl. Phys. A* **944**, 1 (2015).
- [4] S. A. Giuliani, Z. Matheson, W. Nazarewicz, E. Olsen, P.-G. Reinhard, J. Sadhukhan, B. Schuetrumpf, N. Schunck, and P. Schwerdtfeger, *Rev. Mod. Phys.* **91**, 011001 (2019).
- [5] W. Nazarewicz, *Nat. Phys.* **14**, 537 (2018).
- [6] K. Hagino, *Assoc. Asia Pacific Phys. Soc. Bull.* **29**, 31 (2019).
- [7] K. Morita *et al.*, *J. Phys. Soc. Jpn.* **73**, 2593 (2004); K. Morita, *ibid.* **76**, 045001 (2007); **81**, 103201 (2012).
- [8] W. D. Myers and W. J. Swiatecki, *Nucl. Phys.* **81**, 1 (1966).
- [9] A. Sobiczewski, F. A. Gareev, and B. N. Kalinkin, *Phys. Lett.* **22**, 500 (1966).
- [10] R. Yanez, W. Loveland, L. Yao, J. S. Barrett, S. Zhu, B. B. Back, T. L. Khoo, M. Alcorta, and M. Albers, *Phys. Rev. Lett.* **112**, 152702 (2014).
- [11] C. E. Düllmann, *EPJ Web Conf.* **163**, 00015 (2017).
- [12] K. Satou, H. Ikezoe, S. Mitsuoka, K. Nishio, C. J. Lin, and S. C. Jeong, *Phys. Rev. C* **73**, 034609 (2006).
- [13] P. Möller, J. R. Nix, P. Armbruster, S. Hofmann, and G. Münzenberg, *Z. Phys. A* **359**, 251 (1997).
- [14] G. Mohanto, D. J. Hinde, K. Banerjee, M. Dasgupta, D. Y. Jeung, C. Simenel, E. C. Simpson, A. Wakhle, E. Williams, I. P. Carter, K. J. Cook, D. H. Luong, C. S. Palshetkar, and D. C. Rafferty, *Phys. Rev. C* **97**, 054603 (2018).
- [15] C. Simenel, D. J. Hinde, R. du Rietz, M. Dasgupta, M. Evers, C. J. Lin, D. H. Luong, and A. Wakhle, *Phys. Lett. B* **710**, 607 (2012).
- [16] K. Sekizawa, *Front. Phys.* **7**, 20 (2019).
- [17] P. D. Stevenson and M. C. Barton, *Prog. Part. Nucl. Phys.* **104**, 142 (2019).
- [18] C. Simenel and A. S. Umar, *Prog. Part. Nucl. Phys.* **103**, 19 (2018).
- [19] T. Nakatsukasa, K. Matsuyanagi, M. Matsuo, and K. Yabana, *Rev. Mod. Phys.* **88**, 045004 (2016).
- [20] C. Simenel, *Eur. Phys. J. A* **48**, 152 (2012).
- [21] J. W. Negele, *Rev. Mod. Phys.* **54**, 913 (1982).
- [22] A. Wakhle, C. Simenel, D. J. Hinde, M. Dasgupta, M. Evers, D. H. Luong, R. du Rietz, and E. Williams, *Phys. Rev. Lett.* **113**, 182502 (2014).
- [23] A. S. Umar and V. E. Oberacker, *Nucl. Phys. A* **944**, 238 (2015).
- [24] V. E. Oberacker, A. S. Umar, and C. Simenel, *Phys. Rev. C* **90**, 054605 (2014).
- [25] K. Sekizawa and K. Yabana, *Phys. Rev. C* **93**, 054616 (2016).
- [26] C. Shen, G. Kosenko, and Y. Abe, *Phys. Rev. C* **66**, 061602(R) (2002).
- [27] W. J. Swiatecki, K. Siwek-Wilczynska, and J. Wilczynski, *Acta Phys. Pol. B* **34**, 2049 (2003); *Phys. Rev. C* **71**, 014602 (2005).
- [28] Y. Aritomo and M. Ohta, *Nucl. Phys. A* **744**, 3 (2004).
- [29] V. I. Zagrebaev and W. Greiner, *Nucl. Phys. A* **944**, 257 (2015).
- [30] K. Sekizawa and K. Yabana, *Phys. Rev. C* **88**, 014614 (2013).
- [31] K. Sekizawa and K. Yabana, *Phys. Rev. C* **90**, 064614 (2014).
- [32] K. Sekizawa, *Phys. Rev. C* **96**, 014615 (2017).
- [33] K.-H. Kim, T. Otsuka, and P. Bonche, *J. Phys. G* **23**, 1267 (1997).
- [34] D. J. Hinde, D. Y. Jeung, E. Prasad, A. Wakhle, M. Dasgupta, M. Evers, D. H. Luong, R. du Rietz, C. Simenel, E. C. Simpson, and E. Williams, *Phys. Rev. C* **97**, 024616 (2018).
- [35] D. J. Hinde, M. Dasgupta, J. R. Leigh, J. P. Lestone, J. C. Mein, C. R. Morton, J. O. Newton, and H. Timmers, *Phys. Rev. Lett.* **74**, 1295 (1995).
- [36] D. J. Hinde, M. Dasgupta, J. R. Leigh, J. C. Mein, C. R. Morton, J. O. Newton, and H. Timmers, *Phys. Rev. C* **53**, 1290 (1996).
- [37] K. Nishio, H. Ikezoe, S. Mitsuoka, I. Nishinaka, Y. Nagame, Y. Watanabe, T. Ohtsuki, K. Hirose, and S. Hofmann, *Phys. Rev. C* **77**, 064607 (2008).
- [38] K. Nishio, H. Ikezoe, S. Mitsuoka, and J. Lu, *Phys. Rev. C* **62**, 014602 (2000).
- [39] T. Tanaka, Y. Narikiyo, K. Morita, K. Fujita, D. Kaji, K. Morimoto, S. Yamaki, Y. Wakabayashi, K. Tanaka, M. Takeyama, A. Yoneda, H. Haba, Y. Komori, S. Yanou, B. J.-P. Gall, Z. Asfari, H. Faure, H. Hasebe, M. Huang, J. Kanaya, M. Murakami, A. Yoshida, T. Yamaguchi, F. Tokanai, T. Yoshida, S. Yamamoto, Y. Yamano, K. Watanabe, S. Ishizawa, M. Asai, R. Aono, S. Goto, K. Katori, and K. Hagino, *J. Phys. Soc. Jpn.* **87**, 014201 (2018).
- [40] K. Hagino, *Phys. Rev. C* **98**, 014607 (2018).
- [41] K. Washiyama and D. Lacroix, *Phys. Rev. C* **78**, 024610 (2008).
- [42] C. Simenel, A. S. Umar, K. Godbey, M. Dasgupta, and D. J. Hinde, *Phys. Rev. C* **95**, 031601(R) (2017).
- [43] M. Dasgupta, D. J. Hinde, N. Rowley, and A. M. Stefanini, *Annu. Rev. Nucl. Part. Sci.* **48**, 401 (1998).
- [44] A. B. Balantekin and N. Takigawa, *Rev. Mod. Phys.* **70**, 77 (1998).
- [45] K. Hagino and N. Takigawa, *Prog. Theor. Phys.* **128**, 1061 (2012).
- [46] B. B. Back, H. Esbensen, C. L. Jiang, and K. E. Rehm, *Rev. Mod. Phys.* **86**, 317 (2014).
- [47] G. Montagnoli and A. M. Stefanini, *Eur. Phys. J. A* **53**, 169 (2017).
- [48] T. Cap, K. Siwek-Wilczynska, and J. Wilczynski, *Phys. Rev. C* **83**, 054602 (2011).
- [49] K. Siwek-Wilczynska, T. Cap, M. Kowal, A. Sobiczewski, and J. Wilczynski, *Phys. Rev. C* **86**, 014611 (2012).
- [50] Y. Abe, D. Boilley, B. G. Giraud, and T. Wada, *Phys. Rev. E* **61**, 1125 (2000).
- [51] M. Kowal, P. Jachimowicz, and J. Skalski, *arXiv:1203.5013*.
- [52] Y. Hashimoto and G. Scamps, *Phys. Rev. C* **94**, 014610 (2016).
- [53] P. Magierski, K. Sekizawa, and G. Wlazłowski, *Phys. Rev. Lett.* **119**, 042501 (2017).